J. Microbiol. Biotechnol. (2008), **18**(2), 299–307

JOURNAL OF MICROBIOLOGY AND BIOTECHNOLOGY

Expression and Purification of Intact and Functional Soybean (*Glycine max*) Seed Ferritin Complex in *Escherichia coli*

Dong, Xiangbai, Bo Tang, Jie Li, Qian Xu, Shentong Fang, and Zichun Hua*

The State Key Laboratory of Pharmaceutical Biotechnology and Department of Biochemistry, College of Life Sciences, Nanjing University, Nanjing 210093, P. R. China

Received: April 7, 2007 / Accepted: July 2, 2007

Soybean seed ferritin is essential for human iron supplementation and iron deficiency anemia prevention because it contains abundant bioavailable iron and is frequently consumed in the human diet. However, it is poorly understood in regards its several properties, such as iron mineralization, subunit assembly, and protein folding. To address these issues, we decided to prepare the soybean seed ferritin complex *via* a recombinant DNA approach. In this paper, we report a rapid and simple *Escherichia coli* expression system to produce the soybean seed ferritin complex. In this system, two subunits of soybean seed ferritin, H-2 and H-1, were encoded in a single plasmid, and optimal expression was achieved by additionally coexpressing a team of molecular chaperones, trigger factor and GroEL-GroES. The His-tagged ferritin complex was purified by Ni^{2+} affinity chromatography, and an intact ferritin complex was obtained following His-tagged enterokinase (His-EK) digestion. The purified ferritin complex synthesized in *E. coli* demonstrated some reported features of its native counterpart from soybean seed, including an apparent molecular weight, multimeric assembly, and iron uptake activity. We believe that the strategy described in this paper may be of general utility in producing other recombinant plant ferritins built up from two types of subunits.

Keywords: Ferritin, soybean seed, molecular chaperone, Ni^{2+} affinity chromatography, *Escherichia coli*

The iron storage protein ferritin is widely distributed in animals, plants, and microorganisms. It can sequester cellular excess iron for later utilization when needed, and therefore plays a pivotal role in maintaining iron homeostasis [1, 26]. Ferritin has a highly conserved molecular architecture in all organisms. It is generally built up from 24 identical or very similar subunits with variable ratios [7, 16, 25]. Every subunit contains a four-helix bundle (helices A, B, C, and D) and a fifth short helix (helix E). Two ferritin subunit types, H (heavy) and L (light), have been characterized in vertebrates, and *in vitro* formation of the protein nanoparticle was demonstrated using recombinant human ferritin H and L chains produced from *E. coli* [2, 22]. The H subunit has ferroxidase activity and catalyzes the oxidation of iron (II) [12, 13], whereas the L subunit promotes the nucleation and storage of iron (III) [15].

Plant ferritin is synthesized as a subunit precursor with a unique two-domain *N*-terminal sequence, the "transit peptide" (TP) and the following "extension peptide" (EP) [21]. Following transport to plastids, the TP is excised from the mature protein, possibly by active oxygen species during iron exchange. For the small subunit, a short *C*-terminal amino acid sequence will be further cleaved by an unknown site-specific protease [19]. Ferritin purified from dried soybean seed is made of two subunits of 26.5 and 28 kDa, which are designated H-1 and H-2, respectively [19]. The H-1 subunit was initially supposed to be derived from H-2. Subsequent studies indicated that H-1 and H-2 are encoded by two distinct genes, *SferH-1* (GenBank Accession No. M64337) and *SferH-2* (GenBank Accession No. AB062754), respectively, although they share 82% amino acid sequence identity with each other. Compared with their own precursors of 32 kDa, H-1 is devoid of the *N*-terminal TP domain and the *C*-terminal E helix consisting of 16 amino acid residues, whereas H-2 is lacking of its *N*-terminal TP domain only [19].

Iron is an essential element for human being and a lack of iron in the human body can lead to iron deficiency anemia, which is one of the most prevalent nutritional diseases in the developing and even industrialized countries [10]. Soybean seed ferritin is a principal source of dietary iron and rich in bioavailable iron, rendering it essential for human iron supplementation and iron deficiency anemia

*Corresponding author
Phone: 86-25-83324605; Fax: 86-25-83324605;
E-mail: zchua@nju.edu.cn

prevention [5]. However, it is poorly understood in regards its iron mineralization, subunit assembly, and protein folding. Considering it is a well-characterized member of the plant ferritin family and natively composed of two subunits, we are especially interested in investigating the structure-function relationship of the complex. The first step of the project was to prepare the soybean seed ferritin complex from natural material or *via* recombinant DNA technology. However, production of native soybean seed ferritin was costly and time-consuming owing to it requiring expensive reagents and multistep chromatography [11, 24]. Therefore, it is necessary to establish a timesaving and inexpensive *E. coli* expression system to produce the soybean seed ferritin complex, with high yield and high purity, for further structural biology study.

In this study, we developed a rapid and simple system to produce soybean seed ferritin in *E. coli*. We examined the influence of individual subunit and molecular chaperones, trigger factor and GroEL-GroES, on the solubility and stability of the recombinant soybean seed ferritin complex. Recombinant ferritin was expressed in the amino terminal hexahistidine fusion protein form and purified by one-step Ni^{2+} affinity chromatography. Following His-tagged enterokinase (His-EK) digestion, the intact ferritin complex was separated from the fusion tag and its iron uptake activity was verified by an iron (II) oxidation-based iron incorporation experiment.

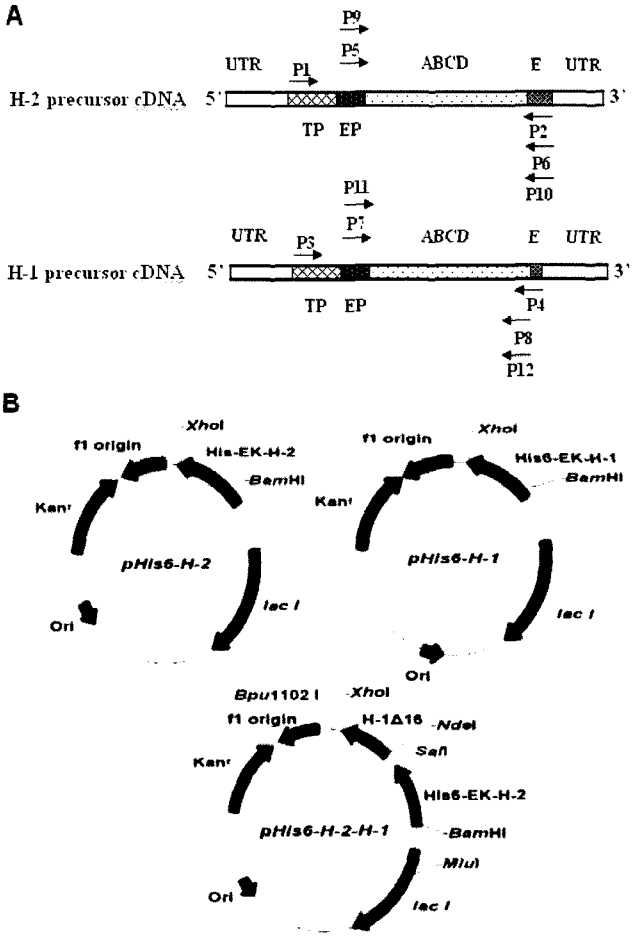

Fig. 1. Constructions of soybean seed ferritin expression vectors. **A.** Schematic diagrams of two full-length cDNAs encoding the H-2 and H-1 subunits precursors, respectively. UTR, untranslated region; TP, the sequence encoding the transit peptide responsible for plasmid targeting of ferritin precursors; EP, the sequence encoding extension peptide found especially in the *N*-terminus of the mature plant ferritin subunits; A, B, C, D, and E, the sequences encoding A, B, C, D, and E helixes in ferritin subunits or their precursors, respectively; P1-P12, primers used to construct ferritin expression vectors (their sequences and corresponding PCR amplicons are described in Materials and Methods). **B.** Schematic diagrams of recombinant pHis6-H-2, pHis6-H-1, and pHis6-H-2-H-1, used to express the H-2 subunit, the H-1 subunit, and both of them synchronously, respectively.

Materials and Methods

Cloning of Two cDNAs Encoding the Full-Length Soybean Seed Ferritin H-1 and H-2 Subunit Precursors

Total RNA was extracted from 10-day-old soybean seedlings using TRIzol Reagent according to the manufacturer's instructions (Invitrogen, Carlsbad, CA, U.S.A.). These seedlings were grown in a greenhouse until each of them contained developed bifoliates, an epicotyl, and a terminal bud. RNA was treated with DNase I (Promega, Madison, WI, U.S.A.). The first strand of cDNAs was synthesized from total RNA (5 μg) using oligo(dT) primer and SuperScript II Reverse Transcriptase according to the manufacturer's instructions (Invitrogen, Carlsbad, CA, U.S.A.). PCR was performed using high fidelity thermostable polymerase Pyrobest (TaKaRa, Dalian, China). Unless described elsewhere, the program for PCR in this study was 94°C for 5 min, followed by 28 cycles consisting of 94°C for 30 s, 56°C for 30 s, and 72°C for 1 min, and a final extension at 72°C for 10 min. Primers P1 (5'-ATGGCCCTTTCTTG-CTCCAAAG-3') and P2 (5'-TTATACATGATCTTCATCGT-3') were used to amplify the cDNA encoding the full-length H-2 subunit precursor comprising its mature region and *N*-terminal TP domain (Fig. 1A). Similarly, primers P3 (5'-ATGGCTCTTGCTCCATCC-AAAG-3') and P4 (5'-CTAATCAAGAAGTCTTTGATC-3') were used to amplify the cDNA encoding the full-length H-1 subunit precursor containing its mature region, *N*-terminal TP domain, and *C*-terminal E helix (Fig. 1A). Two resulting full-length cDNAs, each encoding one subunit precursor, were cloned into the pMD18-T vector (TaKaRa, Dalian, China) and determined by DNA sequencing.

Construction of Soybean Seed Ferritin Expression Vectors pHis6-H-2, pHis6-H-1, and pHis6-H-2-H-1

For the construction of pHis6-H-2 (Fig. 1B), the DNA sequence encoding the H-2 subunit was amplified using primers P5 (5'-TGCGGATCCGACGACGACGACAAGGCTTCAAATGCACC-CGCACC-3') and P6 (5'-CAGCTCGAGTTATACATGATCTTC-ATCGT-3') (Fig. 1A). P5 and P6 contained BamHI and XhoI restriction sites (underlined), respectively. The resulting DNA fragment, which lacked of the TP sequence, was inserted to the BamHI and XhoI sites in pET28a (Novagen, Madison, WI, U.S.A.). For the construction of pHis6-H-1 (Fig. 1B), the DNA sequence encoding the H-1 subunit was amplified using primers P7 (5'-TGCGGATCC-GACGACGACGACAAGTCAACGGTGCCTCTCACT-3') and P8 (5'-CCGCTCGAGTTACCTTCTCAACTGAGCCAC-3') (Fig. 1A). P7 and P8 carried BamHI and XhoI sites (underlined), respectively.

sequence, was cloned to the BamHI and XhoI sites in pET28a. The recombinant H-2 and H-1 subunits were expressed in His-tag fusion form. To facilitate the removal of the fused tag, an additional DNA sequence of 5'-gacgacgacgacaag-3' (framed), which encoded an enterokinase (EK) cleavage site consisting of 5 amino acid residues (DDDDK), was embedded at the 5' ends of primers 5 and 7 (framed), respectively.

The pACYCDuet-1 vector (Novagen, Madison, WI, U.S.A.) was used to construct pHis6-H-2-H-1 (Fig. 1B). There are two multiple cloning sites (MCS) in pACYCDuet-1, each of which is preceded by a T7 promoter/lac operator. Primers P9 (5'-TGCGGATCCG-GACGACGACGACAAG GCTTCAAATGCACCCGCACC-3') and P10 (CAGGTCGACT ATACATGATCTTCATCGT-3'), and primers P11 (CGCCATATGTCAACGGTGCCTCTCACT-3') and P12 (CAG-CTCGAGTTACCTTCTCAACTGAGCCAC-3') were used to amplify DNA fragments encoding the H-2 and H-1 subunits, respectively (Fig. 1A). P9, P10, P11, and P12 possessed BamHI, SalI, NdeI, and XhoI sites (underlined), respectively. The resultant H-2- and H-1-encoding fragments, each of which was lacking of its TP sequence, were respectively cloned into the BamHI/SalI and NdeI/XhoI sites in pACYCDuet-1 to generate a recombinant plasmid pACYCDuet-1/His6-H-2/H-1, in which H-2 was designed to be expressed in His-tag fusion form and H-1 in native form. For the release of intact H-2, an EK recognition site (DDDDK) was induced between His-tag and H-2. For the conversion of chloramphenicol resistance to kanamycin resistance, a 2.0-kb MluI/Bpu1102 I fragment, comprising the expression cassette of both His6-H-2 and H-1 as well as the partial encoding region of lac I, was excised from pACYCDuet-1/His6-H-2/H-1 and ligated with pET28a, which had been digested with MluI and Bpu1102 I. The final recombinant plasmid was designated pHis6-H-2-H-1.

Expression, Quantification, and Solubility Analysis of Recombinant Ferritin and Its Subunits

Ferritin-expressing plasmids pHis6-H-2, pHis6-H-1, and pHis6-H-2-H-1 were respectively transformed into BL21 (DE3) (Novagen, Madison, WI, U.S.A.), and positive clones were screened on LB agar plates containing kanamycin (50 mg/l) at 37°C. Sixteen h later, a single colony was inoculated into 1 l of LB broth containing kanamycin (50 mg/l) and grown with vigorous shaking (250 rpm) overnight at 37°C. When the optical density at 600 nm (OD_{600}) reached 0.8, IPTG (Promega, Madison, WI, U.S.A.) was added to induce the expression of target protein at a final concentration of 0.5 mM. Three h later, cells were harvested by spinning at 5,000 rpm for 5 min. Cell pellets were resuspended in 50 ml of lysis buffer (50 mM sodium phosphate, 0.3 M NaCl, pH 8.0) and lysed by ultrasonic liquid processor (Sonic Dismembrator 550; Fisher Scientific, Pittsburgh, PA, U.S.A.) for 30 min in an ice bath. The supernatant was clarified by centrifugation at 12,000 rpm for 15 min at 4°C and stored at −70°C, while an aliquot of aqueous sample was analyzed by 12% SDS-PAGE. The Coomassie blue-stained SDS-PAGE gel was photographed with a UVP white/UV transilluminator, and the intensities of protein bands were quantified with Grab-it 2.5 and Gelwork 3.01 (UVP; Upland, CA, U.S.A.).

The solubility of recombinant ferritin and its subunits was analyzed using the method described previously [27]. Briefly, cultures were adjusted to the same OD_{600} and cells from 3 ml of adjusted cultures were disrupted by sonic oscillation in 300 μl of iced lysis buffer. The crude lysate was separated into total, soluble, and insoluble fractions (each 150 μl), and 20 μl of aqueous sample of each fraction was resolved by 12% SDS-PAGE. Gel staining, scanning, and protein band quantification were conducted as described above. The solubility was determined as soluble target protein/total expressed target protein×100%.

Coexpression of Recombinant Ferritin or Its Subunits with Molecular Chaperones

Plasmid pG-Tf2, a gift from Dr. Hideki Yanagi (HSP Research Institute, Japan), was chloramphenicol-resistant and compatible with plasmid containing the ColE1 origin [20]. It could synchronously express trigger factor (TF) and GroEL-GroES chaperones under the control of the tetracycline inducible promoter Pzt-1. To enhance the solubility of recombinant ferritin or its subunits, plasmids pHis6-H-2, pHis6-H-1, and pHis6-H-2-H-1 were respectively transformed into BL21 (DE3) together with pG-Tf2, and positive clones were screened on LB agar plates containing kanamycin (50 mg/l) and chloramphenicol (34 mg/l). A culture from a single colony was grown at 37°C. When the OD_{600} reached around 0.6, tetracycline was added to induce chaperones expression at a final concentration of 10 μg/l. Twenty min later, IPTG was added to induce the expression of target protein at a final concentration of 0.5 mM. The culture was incubated at 37°C for an additional 3 h and harvested cells were analyzed by 12% SDS-PAGE.

Purification and Identification of Recombinant Ferritin and Its Subunits

His-Select HC nickel affinity gel was used to purify recombinant ferritin and its subunits according to the manufacturer's instructions (Sigma, St. Louis, MO, U.S.A.). One colony of host strain harboring pHis6-H-2, pHis6-H-1, or pHis6-H-2-H-1 together with pG-Tf2 was cultured in LB broth containing kanamycin (50 mg/l) and chloramphenicol (34 mg/l). Cells from 1 l of IPTG and tetracycline induced cultures were harvested and processed using the methods mentioned above. The resulting supernatant containing the expressed ferritin or its subunits was loaded onto a 3-ml Ni^{2+} affinity gel column, which was pre-equilibrated with buffer A (50 mM sodium phosphate, 0.3 M NaCl, 10 mM imidazole, pH 8.0). Nonspecific binding proteins were washed with buffer B (50 mM sodium phosphate, 0.3 M NaCl, 10–50 mM imidazole, pH 8.0). Recombinant ferritin or its subunits were eluted with buffer C (50 mM sodium phosphate, 0.3 M NaCl, 50–250 mM imidazole, pH 8.0).

The eluted fraction was dialyzed against buffer D (20 mM Tris-HCl, 200 mM NaCl, pH8.0) to remove imidazole. After dialysis, the protein concentration was measured by BCA kit (Pierce, Rockford, IL, U.S.A.) with bovine serum albumin (BSA) as reference, and recombinant ferritin or its subunits was incubated with His-tagged enterokinase (His-EK) (1:5,000; w/w) overnight at 16°C, which was prepared as described previously [6]. The digested solution was applied to a Ni^{2+} affinity column to deplete His-tag and His-EK, and then intact ferritin or its subunits were obtained as the flowthrough.

The yield and purity of chimeric and intact ferritins were quantified by BCA kit and densitometric analysis of SDS-PAGE. The recombinant ferritin complex was identified using Western blotting, which was performed according to standard protocol. Around 5–10 μg of target protein was separated by 12% SDS-PAGE and electroblotted to nitrocellulose membranes (Hybond C; Amersham, Piscataway, NJ, U.S.A.). Mouse polyclonal antiserum against soybean ferritin was used as the primary antibody (1:1,000; v/v), which was

prepared as described by Laulhere *et al.* [11]. HRP-conjugated rabbit anti-mouse IgG (Santa Cruz, CA, USA) was used as the secondary antibody (1:3,000; v/v). The Western Lighting Chemiluminescence Reagent Plus (PerkinElmer, Fermont, CA, U.S.A.) was used to detect signals on x-ray films.

Iron Incorporation Analysis of Recombinant Ferritin

Apoferritin was obtained using methods described by Chasteen and Theil [3]. Purified ferritin or its subunits were dialyzed against 50 mM HEPES/NaOH buffer (pH 7.0) containing 1% thioglycolic acid, followed by successive changes of HEPES buffer with (0.1%) and without thioglycolic acid. Protein was then dialyzed against HEPES buffer containing 13 g/l of Chelex-100 (Sigma, St. Louis, MO, U.S.A.) and 0.2 M NaCl and finally against deionized water.

Iron uptake measurement was performed according to the protocol described by Masuda *et al.* [19]. Briefly, apoferritin (0.1 μM) was mineralized using freshly prepared ferrous sulfate (0.1 M) dissolved in 0.1 M HEPES/NaOH buffer (pH 7.0) at room temperature. Iron incorporation by recombinant ferritin was monitored by measuring the absorbance at 310 nm using a UV spectrophotometer (U3000; Hitachi, Tokyo, Japan).

Results

Generation of Engineered Bacteria Strains Expressing Soybean Seed Ferritin or Its Subunits

To generate soybean seed ferritin-engineered bacteria, three different expression vectors, pHis6-H-2, pHis6-H-1, and pHis6-H-2-H-1 (Fig. 1B), were constructed. The former two plasmids were used to express the H-2 and H-1 subunits, respectively, and the latter was used to express the H-2 and H-1 subunits simultaneously. Transformants were screened by antibiotics selection (kanamycin) and validated by PCR analysis, restriction digestion, and DNA sequencing in turn. Subsequently, the recombinant expression plasmids were transformed into BL21 (DE3) by electroporation, individually or together with pG-Tf2, and the engineered ferritin-producing strains were thus obtained.

Analysis of Expression of Recombinant H-2 and H-1 Subunits

Two colonies of host strain, each harboring either pHis6-H-2 or pHis6-H-1, were cultured in LB broth containing kanamycins (50 mg/l), respectively. Upon IPTG induction, recombinants H-2 and H-1 were expressed with apparent molecular masses of around 32 kDa and 30.5 kDa (Fig. 2A) respectively, each of which was 4 kDa larger than the corresponding subunit from soybean seed ferritin. The additional 4 kDa was derived from the *N*-terminal fused partner consisting of a proximal His-tag and distal peptide fragment expressed by pET 28, which was in-frame within the H1 or H2 construct (Fig. 1B). This result suggested that both His6-H-2 and His6-H-1 were successfully expressed. However, both of them were mainly deposited as inclusion bodies. Solubility analysis showed that 19% of His6-H-2 and 4% of His6-H-1 appeared in the soluble fractions (Fig. 2A).

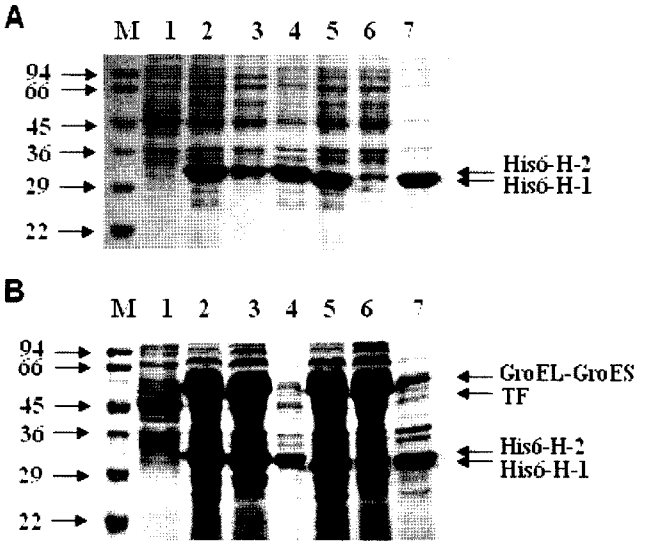

Fig. 2. SDS-PAGE analysis of the solubilities of recombinants His6-H-2 and His6-H-1.

A. Solubility analysis of recombinants His6-H-2 and His6-H-1. Cell pellets from 3 ml of cultures were disrupted by sonic oscillation in 300 μl of iced lysis buffer. The crude lysate was separated into total, soluble, and insoluble fractions (each 150 μl), and 20 μl of aqueous sample of each fraction was resolved by 12% SDS-PAGE. Lane 1, total bacterial protein from IPTG-induced BL21(DE3) harboring pET28a; lanes 2–4, total, supernatant, and insoluble fractions from IPTG-induced BL21(DE3) carrying pHis6-H-2, respectively; lanes 5–7, total, supernatant, and insoluble fractions from IPTG-induced BL21(DE3) carrying pHis6-H-1, respectively; lane M, protein markers and their corresponding molecular masses (kDa). **B.** Solubility analysis of His6-H-2 and His6-H-1 coexpressed with GroEL-GroES and TF. Samples were prepared as described above and resolved by 12% SDS-PAGE. Lane 1, total bacterial protein from IPTG-induced BL21(DE3) harboring pET28a; lanes 2–4, total, supernatant, and insoluble fractions from Tet/IPTG-induced BL21(DE3) carrying pHis6-H-2 and pG-Tf2, respectively; lanes 5–7, total, supernatant, and insoluble fractions from Tet/IPTG-induced BL21(DE3) carrying pHis6-H-1 and pG-Tf2, respectively; lane M, protein markers and their corresponding molecular masses (kDa).

It has been previously reported that coexpression with TF and GroEL-GroES could significantly enhanced the solubility of target proteins [8, 20]. To determine whether these chaperones ameliorated the aggregation of heterogeneously overexpressed H-2 and H-1 subunits, His6-H-2 and His6-H-1 were coexpressed with TF and GroEL-GroES, respectively. The results showed that molecular chaperone coexpression could greatly increase the solubility of H-2 from 19% to 85%, but it exhibited subtle influence on the solubility of the H-1 subunit from 4% to 39% (Fig. 2B).

Purification of Recombinant H-2 and H-1 Subunits

To purify recombinants His6-H-2 and His6-H-1, one-step Ni^{2+} affinity chromatography was employed. Recombinant His6-H-2 was stable and eluted by 250 mM imidazole (Fig. 3A). Compared with His6-H-2, His6-H-1 was

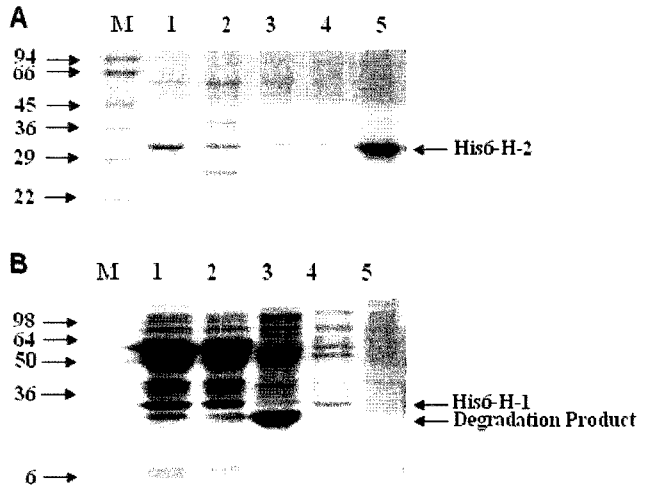

Fig. 3. Purification of recombinants His6-H-2 and His6-H-1 by Ni^{2+} affinity gel chromatography.

A. SDS-PAGE analysis of purified His6-H-2. Lane 1, total soluble proteins from IPTG-induced BL21(DE3) harboring pHis6-H-2; lane 2, flowthrough of Ni^{2+} column; lanes 3–5, the eluents with 25, 50, and 250 mM imidazole, respectively; lane M, protein markers and their corresponding molecular masses (kDa). **B.** SDS-PAGE analysis of purified His6-H-1. Lane 1, total soluble proteins from IPTG-induced BL21(DE3) carrying pHis6-H-1 and pG-Tf2; lane 2, flowthrough of Ni^{2+}-column; lanes 3–5, the eluents with 25, 50, and 250 mM imidazole, respectively; lane M, protein markers and their corresponding molecular masses (kDa).

difficult to purify. The overwhelming His6-H-1 appeared in the elution fraction by 25 mM imidazole, but was contaminated by endogenous *E. coli* proteins. Moreover, His6-H-1 was unstable and inclined to degrade into a small derivative of 22 kDa, the identity of which was confirmed by Western blotting (data not shown, Fig. 3B). In short, recombinant His6-H-2 was stable and easy to purify, whereas recombinant His6-H-1 was prone to aggregation and degradation.

Coexpression with the H-2 Subunit Confers Solubility and Stability to the H-1 Subunit

In soybean seed, the H-2 and H-1 subunits assemble into a large heteropolymer, indicating H-2 in the complex might assist in the stability of H-1 and facilitate the assembly of soybean seed ferritin. Considering this possible interaction, an expression plasmid, pHis6-H-2-H-1, was constructed, in which H-2- and H-1-encoding DNA fragments were placed individually under the control of the T7 promoter/lac operator. Upon IPTG induction, the strain harboring pHis6-H-2-H-1 would express simultaneously the H-1 and H-2 subunits. Coexpression with the H-2 subunit obviously improved the solubility of the H-1 subunit from 4% to 18% (Fig. 4A). To further improve the solubility of recombinant His6-H2/H-1, we coexpressed a team of chaperones, TF and GroEL-GroES. Solubility analysis showed that coexpression with both H-2 and chaperones remarkably enhanced the solubility of H-1 (89%), which reached a level almost comparable to that of H-2 (93%) (Fig. 4B).

Preparation of Intact Recombinant H-2/H-1 Complex

Recombinant His6-H-2/H-1 coexpressed with TF and GroEL-GroES was successfully purified through one-step Ni^{2+} affinity chromatography. After dialysis, subsequent digestion with His-EK, and the following removal of His-tag and His-EK with Ni^{2+} resin, an intact recombinant H-2/H-1 complex was obtained with purity around 96% (Table 1). Sixty-five mg of intact ferritin was finally produced from 1 l of bacterial culture (Table 1). Purified H-2/H-1 migrated as about 28-kDa and 26.5-kDa bands in SDS-PAGE (Fig. 4C). Its densitometric analysis showed that H-2 and H-1 represented 71.8% and 28.2%, respectively. The chimeric His6-H-2/H-1 and intact H-2/H-1 complex were confirmed by Western blotting (Fig. 4D).

To determine whether recombinant His6-H-2/H-1 and its purified product H-2/H-1 could spontaneously form a heteropolymer, a native PAGE was carried out. The result showed that both recombinant His6-H-2/H-1 and intact H-2/H-1 appeared as one single band with slow mobility, indicating that both His6-H-2/H-1 and H-2/H-1 were able to assemble into a large multimeric heteropolymer (Fig. 4E).

Recombinant Ferritin Shows Significant Iron Uptake Activity

To investigate whether recombinant ferritin possesses ferroxidase activity, an iron (II) oxidation-based iron incorporation experiment was carried out. The apoferritin, acquired as the recombinant H2/H1 complex, was detected for its iron (II) uptake activity in the presence of oxygen and 1,000-fold molar excess of Fe^{2+} (0.1 mM ferrous sulfate and 0.1 μM ferritin) at room temperature. Recombinant H-2/H-1 exhibited significant iron uptake activity. Iron (II) oxidation rates were faster in the presence of recombinant ferritin than in the presence of BSA (Fig. 5). The reaction catalyzed by our recombinant ferritin complex showed a sharply hyperbolic curve and reached its plateau phase 175 s after incubation, whereas the progression plots of iron (II) oxidation with or without BSA remained a slightly ascending line during the whole incubation.

DISCUSSION

A number of bacteria and vertebrate ferritins have been produced in *Escherichia coli* [4, 9, 14, 23]. For plant ferritin, its recombinant production is little documented. Masuda *et al.* [18] expressed the 28-kDa H-1 subunit (proposed previously to be the mature H-1 subunit) in *E. coli* and obtained its preliminary crystallization, however, this crystallization in their report just represented the

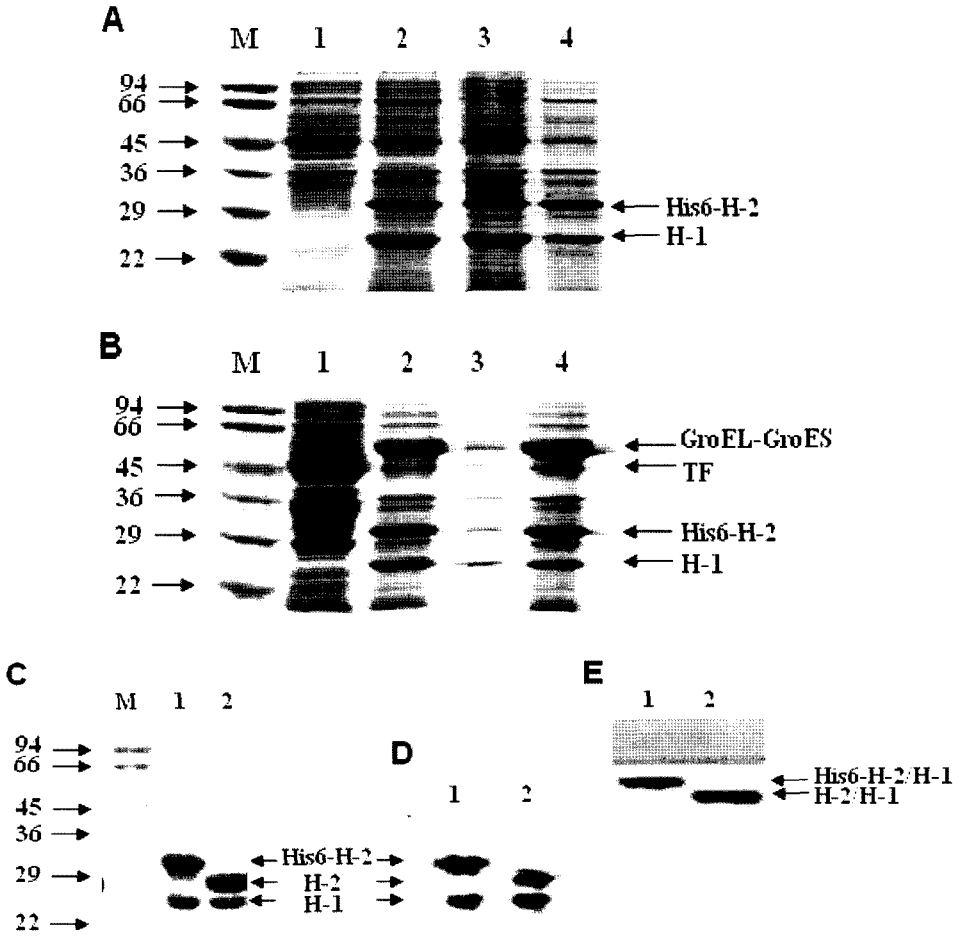

Fig. 4. Expression, purification, and confirmation of recombinant soybean seed ferritin complex.
A. Coexpression with His6-H-2 remarkably improved the solubility and stability of the H-1 subunit. Cell pellets from 3 ml of cultures were disrupted by sonic oscillation in 300 μl of iced lysis buffer. The crude lysate was separated into total, soluble, and insoluble fractions (each 150 μl), and 20 μl of aqueous sample of each fraction was resolved by 12% SDS-PAGE. Lane 1, total bacterial protein from IPTG-induced BL21(DE3) harboring pET28a; lanes 2–4, total, insoluble, and supernatant fractions from IPTG-induced BL21(DE3) carrying pHis6-H-2-H-1; lane M, protein markers and their corresponding molecular masses (kDa). **B**. GroEL-GroES and TF chaperones further enhanced the solubility of coexpressed His6-H-2/H-1 complex. Samples were prepared as described above and resolved by 12% SDS-PAGE. Lane 1, total bacterial protein from IPTG-induced BL21(DE3) harboring pET28a; lanes 2–4, total, insoluble, and supernatant fractions from Tet/IPTG-induced BL21(DE3) carrying pHis6-H-2-H-1 and pG-Tf2, respectively; lane M, protein markers and their corresponding molecular masses (kDa). **C**. A 12% SDS-PAGE analysis of purified His6-H-2/H-1 and H-2/H-1. Lane 1, His6-H-2/H-1 (20 μg); lane 2, H-2/H-1 (20 μg); lane M, protein markers and their corresponding molecular masses (kDa). **D**. Western blotting analysis of purified His6-H-2/H-1 and H-2/H-1. Lane 1, His6-H-2/H-1 (5 μg); lane 2, H-2/H-1 (5 μg). **E**. Native PAGE (8%) analysis of purified His6-H-2/H-1 and H-2/H-1. Lane 1, His6-H-2/H-1 (7 μg); lane 2, H-2/ H-1 (7 μg).

Table 1. Summary of purification of recombinant soybean seed H-2/H-1 complex.

Purification step	Total proteins[a] (mg)	Recovery[b] (100%)
Supernatant[c]	562.9	100.0
No. 1 Ni^{2+} affinity chromatography	78.2	13.9
His-EK[d] digestion	78.2	13.9
No. 2 Ni^{2+} affinity chromatography	65.0	11.6

[a]Total protein concentration was determined by a BCA kit (Pierce, Rockford, IL, U.S.A.) using bovine serum albumin (BSA) as the reference.
[b]Total protein of each step/total protein of supernatant×100%.
[c]From cell lysate of 1 l of IPTG/tetracycline-induced culture.
[d]His-tagged enterokinase.

conformational status of the 28-kDa H-1 subunit alone but not in a ferritin complex. Obviously, the molecular conformation of the mature H-1 subunit (26.5 kDa) is different from that of the 28-kDa H-1 subunit, *e.g.*, recombinant 28-kDa H-1 was soluble and stable, whereas the recombinant mature H-1 subunit in our report, lacking its C-terminal 16 amino acid residues [19], tended to aggregate and degrade. Thus, the reported 28-kDa H-1 subunit cannot fully reflect the factual conformation of the mature H-1 subunit in the ferritin complex, and this makes our current study important and necessary for elucidation of the structure-function relationship of the ferritin complex.

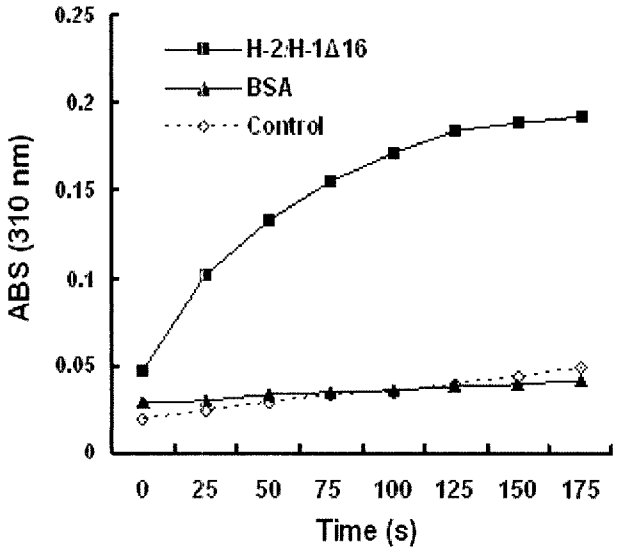

Fig. 5. Kinetics of iron uptake by recombinant ferritin expressed in *E. coli.*

Apoferritin was obtained as a recombinant H-2/H-1 complex and iron uptake measurement was performed as described in Materials and Methods. Experiment was conducted in 0.1 M HEPES-Na, pH 7.0, containing 0.1 μM of recombinant H-2/H-1 and 0.1 mM ferrous sulfate. Iron incorporation by recombinant ferritin and bovine serum albumin (BSA) was monitored by measuring the absorbance at 310 nm. The control indicates the rate of Fe (II) autoxidation.

In the present study, we developed a system for simple and rapid production of soybean seed ferritin in *E. coli.* Using this system, an intact and stable soybean seed ferritin complex was produced with high yield (65 mg from 1 l of induced culture) and purity (around 96%). Recombinant H-2/H-1 successfully assembled into a large multimeric heteropolymer and exhibited the activity of significant iron uptake. In an early study, the iron uptake activity of the native soybean seed ferritin complex was examined using the same method [19]. Progression plots showed that our recombinant H-2/H-1 complex possessed remarkable iron uptake activity (a hyperbolic curve), which was at least comparable to that of natural ferritin purified from dried soybean seed (a sharply ascending line).

Considering the natural heterogeneity of soybean seed ferritin, two strategies were employed during production: one is separate expression (two subunits encoded in two plasmids) and subsequent assembly *in vitro* of H-1 and H-2, and the other is coexpression (two subunits encoded in one plasmid) and spontaneous assembly *in vivo* of H-1 and H-2. The first strategy was abandoned eventually because the H-1 subunit, when heterogeneously overexpressed in *E. coli*, was inclined to aggregate and degrade and therefore could hardly be purified with Ni^{2+} resin, although a His-tag was fused with its *N*-terminus (Fig. 3B). In contrast, the second strategy proved to be simple and feasible. In this strategy, the H-1- and H-2-encoding DNA sequences were intentionally inserted in one plasmid and synchronously expressed upon IPTG introduction. This obviously conferred the solubility and stability to the H-1 subunit. This efficacy was greatly intensified by the introduction of molecular chaperones. As a result, the solubility of H-1 was elevated up to 89%, and the recombinant His6-H-2/H-1 complex was ultimately purified by one-step Ni^{2+} affinity chromatography.

Recombinant 28-kDa H-1 was stable and soluble, whereas recombinant His6-H-1 was prone to aggregation and degradation. The 22-kDa degradation product was also observed by others during the soybean seed germination process [24]. Compared with the 28-kDa H-1 subunit described previously, the H-1 subunit in our paper lacked its *C*-terminal domain consisting of 16 amino acid residues, which was predicted to form a hydrophilic E-helix (Fig. 1A) [17]. The lack of E-helix substantially increases the hydrophobic surface of His6-H-1, which may be responsible for its aggregation and degradation.

The improvement in stability and solubility of the H-1 subunit should be attributed to the assistance of the molecular chaperones and coexistence of the H-2 subunit. When coexpressed with H-2 or TF and GroEL-GroES individually, the solubility of the H-1 subunit was increased 18% or 39%, respectively. On the contrary, when coexpressed with H-2, and TF and GroEL-GroES simultaneously, the solubility of the H-1 subunit was dramatically increased up to 89%, and its stability was greatly improved as well. These results revealed that combined employment of isochronous expression of H-2 and coexpression with TF and GroEL-GroES significantly improved the soluble expression of the H-1 subunit, greatly avoided its degradation, and ultimately increased production of a biologically active soybean seed ferritin complex. The great gain in stability and solubility of the H-1 subunit may be a synergistic consequence of its interaction with the H-2 and assistance of the molecular chaperones.

It should be noted that, besides isochronous expression of H-2 and coexpression of molecular chaperones, the achievement of high-level production of intact soybean seed ferritin also benefited from the application of the *N*-terminal His-tag fusion expression strategy, which is a widely used tactic in the production of genetically engineered proteins. For at least two reasons, we chose this method: one is that the His-tag is small and thus has the potential to produce much more total H-2; and the other is that the *N*-terminal His-tag is removable and able to generate intact H-2 without any remaining amino acid residues when an EK recognition site was introduced between the tag and H-2. In our case, the recombinant His6-H-2/H-1 complex was isolated by one- step Ni^{2+} affinity chromatography, and the cleavage of fused His-tag was accomplished with His-EK. These factors greatly facilitated the production of an intact recombinant soybean seed ferritin complex.

In our research, the recombinant His6-H-2/H-1 complex could spontaneously assemble into a large iron storage protein without the removal of His-tag from His6-H-2, indicating that this affinity tag, when fused at the amino terminal of H-2, had no influence on complex assembly. We speculated that the amino terminal of the H-2 subunit was not embedded in the complex but exposed outside it. Our speculation was partially proven by Lobreaux *et al.* [17]. They proposed a model of three-dimensional structure of the assembled pea seed ferritin by fitting the aligned sequence to the coordinates of human H-chains. In this model, pea seed ferritin subunits were assembled as a compact homopolymer with 432 symmetry, and the *N*-terminal extension of each subunit was exposed on the outside surface of the shell [17].

To our knowledge, this is the first attempt to integrate two-subunit interaction and assistance of molecular chaperones to produce plant ferritin comprising two types of subunits in *E. coli*, although the tactic of a two-subunit coexpression described here has been used previously for the production of human and mouse ferritins [23]. Additionally, it is also the first report on the application of Ni^{2+} affinity chromatography to purify recombinant ferritin. Therefore, our data are a substantial extension to the knowledge of the expression and purification of multimeric ferritin built up from two subunits *via* recombinant DNA approach. More generally, the strategy described in this paper may be suggestive to production of other recombinant ferritin complexes constructed by two types of subunits.

Acknowledgments

We are grateful to Dr. Hideki Yanagi for the plasmid pG-Tf2. This study is supported by funds to Zi-chun Hua from the Chinese National Nature Science Foundation (30330530, 30425009, and 20373026) and the Ministry of Education of China (TRAPOYT1999028418, SRFDP 20030284040).

References

1. Arosio, P. and S. Levi. 2002. Ferritin, iron homeostasis, and oxidative damage. *Free Radic. Biol. Med.* **33:** 457–463.
2. Arosio, P., T. G. Adelman, and J. W. Drysdale. 1978. On ferritin heterogeneity. Further evidence for heteropolymers. *J. Biol. Chem.* **253:** 4451–4458.
3. Chasteen, N. D. and E. C. Theil. 1982. Iron binding by horse spleen apoferritin. A vanadyl (IV) EPR spin probe study. *J. Biol. Chem.* **257:** 7672–7677.
4. Clerte, S., A. Dautant, D. B. Langlois, B. Gallois, Y. Mizunoe, S. N. Wai, and G. Precigoux. 1999. Expression, purification, crystallization and preliminary X-ray diffraction results from *Campylobacter jejuni* ferritin. *Acta Crystallogr. D Biol. Crystallogr.* **55:** 299–301.
5. Davila-Hicks, P., E. C. Theil, and B. Lonnerdal. 2004. Iron in ferritin or in salts (ferrous sulfate) is equally bioavailable in nonanemic women. *Am. J. Clin. Nutr.* **80:** 936–940.
6. Fang, L., Q. M. Sun, and Z. C. Hua. 2004. Expression of recombinant Chinese bovine enterokinase catalytic subunit in *P. pastoris* and its purification and characterization. *Acta Biochim. Biophys. Sin.* **36:** 513–517.
7. Harrison, P. M. and P. Arosio. 1996. The ferritins: Molecular properties, iron storage function and cellular regulation. *Biochim. Biophys. Acta* **1275:** 161–203.
8. Horwich, A. L., G. W. Farr, and W. A. Fenton. 2006. GroEL-GroES-mediated protein folding. *Chem. Rev.* **106:** 1917–1930.
9. Hudson, A. J., S. C. Andrews, C. Hawkins, J. M. Williams, M. Izuhara, F. C. Meldrum, S. Mann, P. M. Harrison, and J. R. Guest. 1993. Overproduction, purification and characterization of the *Escherichia coli* ferritin. *Eur. J. Biochem.* **218:** 985–995.
10. Karimi, M., R. Kadivar, and H. Yarmohammadi. 2002. Assessment of the prevalence of iron deficiency anemia, by serum ferritin, in pregnant women of Southern Iran. *Med. Sci. Monit.* **8:** CR488–CR492.
11. Laulhere, J. P., A. M. Lescure, and J. F. Briat. 1988. Purification and characterization of ferritins from maize, pea, and soya bean seeds. *J. Biol. Chem.* **263:** 10289–10294.
12. Lawson, D. M., A. Treffry, P. J. Artymiuk, P. M. Harrison, S. J. Yewdall, A. Luzzago, G. Cesareni, S. Levi, and P. Arosio. 1989. Identification of the ferroxidase centre in ferritin. *FEBS Lett.* **254:** 207–210.
13. Lawson, D. M., P. J. Artymiuk, S. J. Yewdall, J. M. Smith, J. C. Livingstone, A. Treffry, A. Luzzago, S. Levi, P. Arosio, and G. Cesareni. 1991. Solving the structure of human H ferritin by genetically engineering intermolecular crystal contacts. *Nature* **349:** 541–544.
14. Levi, S., J. Salfeld, F. Franceschinelli, A. Cozzi, M. H. Dorner, and P. Arosio. 1989. Expression and structural and functional properties of human ferritin L-chain from *Escherichia coli*. *Biochemistry* **28:** 5179–5184.
15. Levi, S., S. J. Yewdall, P. M. Harrison, P. Santambrogio, A. Cozzi, E. Rovida, A. Albertini, and P. Arosio. 1992. Evidence of H- and L-chains have co-operative roles in the iron-uptake mechanism of human ferritin. *Biochem. J.* **288(Pt 2):** 591–596.
16. Liu, X. and E. C. Theil. 2005. Ferritins: Dynamic management of biological iron and oxygen chemistry. *Acc. Chem. Res.* **38:** 167–175.
17. Lobreaux, S., S. J. Yewdall, J. F. Briat, and P. M. Harrison. 1992. Amino-acid sequence and predicted three-dimensional structure of pea seed (*Pisum sativum*) ferritin. *Biochem. J.* **288(Pt 3):** 931–939.
18. Masuda, T., B. Mikami, F. Goto, T. Yoshihara, and S. Utsumi. 2003. Crystallization and preliminary X-ray crystallographic analysis of plant ferritin from *Glycine max*. *Biochim. Biophys. Acta* **1645:** 113–115.
19. Masuda, T., F. Goto, and T. Yoshihara. 2001. A novel plant ferritin subunit from soybean that is related to a mechanism in iron release. *J. Biol. Chem.* **276:** 19575–19579.
20. Nishihara, K., M. Kanemori, H. Yanagi, and T. Yura. 2000. Overexpression of trigger factor prevents aggregation of

recombinant proteins in *Escherichia coli*. *Appl. Environ. Microbiol.* **66:** 884–889.
21. Ragland, M., J. F. Briat, J. Gagnon, J. P. Laulhere, O. Massenet, and E. C. Theil. 1990. Evidence for conservation of ferritin sequences among plants and animals and for a transit peptide in soybean. *J. Biol. Chem.* **265:** 18339–18344.
22. Ro, H. S., H. K. Park, M. G. Kim, and B. H. Chung. 2005. *In vitro* formation of protein nanoparticle using recombinant human ferritin H and L chains produced from *E. coli*. *J. Microbiol. Biotechnol.* **15:** 254–258.
23. Rucker, P., F. M. Torti, and S. V. Torti. 1997. Recombinant ferritin: Modulatior of subunit stoichiometry in bacterial expression systems. *Protein Eng.* **10:** 967–973.
24. Sczekan, S. R. and J. G. Joshi. 1987. Isolation and characterization of ferritin from soyabeans (*Glycine max*). *J. Biol. Chem.* **262:** 13780–13788.
25. Theil, E. C. 1987. Ferritin: Structure, gene regulation, and cellular function in animals, plants, and microorganisms. *Annu. Rev. Biochem.* **56:** 289–315.
26. Theil, E. C. 2003. Ferritin: At the crossroads of iron and oxygen metabolism. *J. Nutr.* **133:** 1549S–1553S.
27. Zhao, J. H., Z. Xu, and Z. C. Hua. 2000. Expression of human cardiac-specific homeobox protein in *Escherichia coli*. *Protein Expr. Purif.* **18:** 316–319.